Article

Anion Transporters Based on Noncovalent Balance Including Anion-#, Hydrogen and Halogen Bonding

Wen-Long Huang, Xu-Dong Wang, Sen Li, Rui Zhang, Yu-Fei Ao, Jun Tang, Qi-Qiang Wang, and De-Xian Wang

J. Org. Chem., **Just Accepted Manuscript** • Publication Date (Web): 17 Jun 2019

Anion Transporters Based on Noncovalent Balance Including Anion-π, Hydrogen and Halogen Bonding

Wen-Long Huang,[a,b,#] Xu-Dong Wang,[a,#] Sen Li,[a] Rui Zhang,[c] Yu-Fei Ao,[a] Jun Tang,[c] Qi-Qiang Wang,[a,b,*] and De-Xian Wang[a,b,*]

[a] *Beijing National Laboratory for Molecular Sciences, CAS Key Laboratory of Molecular Recognition and Function, Institute of Chemistry, Chinese Academy of Sciences, Beijing 100190 (China)*

[b] *University of Chinese Academy of Sciences, Beijing 100049 (China)*

[c] *State Key Laboratory of Agrobiotechnology and College of Veterinary Medicine, China Agricultural University, Beijing, 100193, China*

[#] *These authors contribute equally*

qiqiangw@iccas.ac.cn dxwang@iccas.ac.cn

Abstract: Anion transmembrane transport mediated by novel noncovalent interactions is of central interest in supramolecular chemistry. In this work, a series of oxacalix[2]arene[2]triazine-derived transporters **1** and **2** bearing anion-π, hydrogen and halogen bonding sites in rational proximity were designed and synthesized by a one-pot strategy starting from gallic acid ester derivatives and mono- or di-halogen substituted triazines. ^{1}H NMR titrations demonstrated efficient binding of **1** and **2** towards Cl^- and Br^- in solution, giving association constants in the range of 10^2–10^4 M^{-1}. Cooperation of anion-π, hydrogen and halogen bonding was revealed as driving force for anion binding by single crystal structures of two complexes and DFT calculations. Fluorescence assays indicated compounds **1** are efficient chloride transporters with effective concentrations (EC_{50}) falling in the range of 3.1 to 7.4 μM and following an order of **1a** > **1b** > **1c** > **1d**. The contribution of halogen bonding and cooperative noncovalent bonds to ion transport was then discussed. Significantly,

transporters **1** exhibits high anticancer activity. In the presence of **1** and KCl (60 mM), cell survival of HCT116 reduces to 11.9 – 24.9% with IC_{50} values in the range of 52.3 – 66.4 μM.

Introduction

Ion transport across cell membrane represents one of the most essential processes in many living cells. Ion selectivity is the fundamental property of ion-transport proteins, which is achieved by specific noncovalent interactions and stereo-configuration of the binding sites.[1] Inspired by the mysterious function and mechanism of transmembrane proteins, design of synthetic ion transporters based on noncovalent interactions has been one of the most attractive research fields in supramolecular chemistry.[2] While a large amount of artificial cation transporters are known, artificial systems for anion transport are relatively rare.[2] This most probably stemmed from the challenge of anion recognition due to the intrinsic properties of anions such as large size, low electric density and easy polarization, etc. Anion transport has been achieved generally by hydrogen bond-based transporters such as prodigiosin mimics,[3] peptide derivatives,[4] steroidal scaffolds with (thio)urea sidechains,[2e,5] artificial β-barrels,[2b,6] and macrocyclic scaffolds bearing hydrogen bond donors.[7] On the other hand, recent years have witnessed a vast development of halogen bonding and anion-π interactions.[8] Both noncovalent bonds as alternatives of hydrogen bonding show remarkable capability in anion binding and anion recognition, however, halogen bond- and anion-π-based anion channel and transporters are surprisingly limited. Matile and coworkers reported the anion-π oligonaphthalenediimide rods for selective anion transport.[9] Macrocyclic or semi-cage artificial anion transporters comprising electron-deficient aromatic rings were demonstrated by several groups including us.[10] Self-assembled chloride carriers or channels exploiting halogen bonding as driving force were reported independently by Matile's[10b,11] and Zeng's groups.[12] These reports, though still very few, have confirmed the desirable nature of halogen bonding and anion-π interactions for design of anion transport systems.[13] It is worth addressing

that the development of novel noncovalent interactions could in return help us get deep understanding of the mechanism of biological ion transport. For example, the function of anion-π interaction in voltage-dependent response prestin was recently realized by He and Beisel *et al.* They applied a Glt_{ph}-based model and demonstrated the aromatic residues bind intracellular anions through anion-π interactions; such weak interactions are sensitive to voltage and mechanical stimulation and hence can explain the voltage-dependent property of prestin.[14] Therefore it is attractive and important to explore novel noncovalent interactions in design of artificial ion transport system, and to elucidate the contribution and probe the balance of various noncovalent bonds.

Dichloro-substituted oxacalix[2]arene[2]triazine is a typical member of heteracalixaromatics.[15] This preferent host adopts 1,3-alternate conformation in which two triazine rings form an electron-deficient V-shape cleft and shows powerful binding ability to anions through anion-π interactions.[16] The convergent cavity and convenient functionalization of dichloro-substituted oxacalix[2]arene[2]triaizne endow a good molecular platform to achieve cooperativity of various noncovalent interactions. Previously, through introducing hydrogen bond donors on the lower rim of oxacalix[2]arene[2]triazine derivatives, we have shown cooperative anion-π and hydrogen bonding interactions can mediate chloride transmembrane transport.[10a] To manipulate a balance involving more noncovalent interactions, we decided to further introduce halogen bond sites on the upper rim of oxacalix[2]arene[2]triazines to creat a convergent proximity of anion-π pocket with hydrogen and halogen bonding sites (Figure 1). Herein we reported the design and synthesis of such new transporters **1** and **2** and their anion transport studies. The contribution and balance of different noncovalent bonds in mediating the ion transport was highlighted.

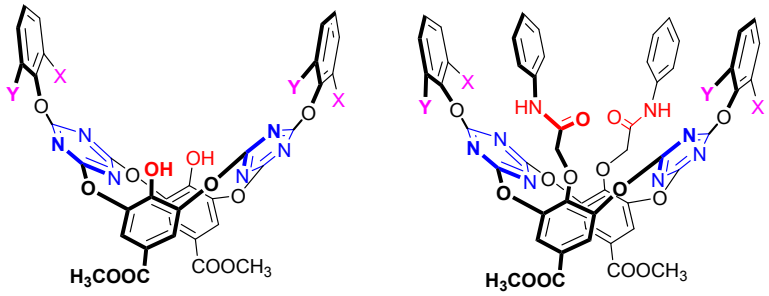

Figure 1. Structures of oxacalix[2]arene[2]triazine-based transporters **1** and **2**.

Results and discussion

Design. Oxacalix[2]arene[2]triaiznes are a good macrocyclic platform suitable for organizing multiple noncovalent interactions in a cooperative manner. In order to manipulate a balance between anion-π, hydrogen and halogen bonding on the macrocyclic scaffold, we decided to incorporate hydrogen bonding sites in the lower rim of benzene rings, and further introduce halogen bonding sites on the upper rim of triazine rings. The hydrogen bonding sites can choose hydroxyl or amide groups, and halogen bonding sites can take bromo or iodo substituted phenyl groups. Considering the macrocyclic geometry and synthetic feasibility, we designed two types of transporters, **1** and **2**. To evaluate whether the V-shape anion-π cavity and the hydrogen and halogen bonding sites are in good convergent proximity and can cooperatively bind anions, e.g. chloride and bromide, we performed DFT calculations on binding of **1b** with Cl^- and Br^- on the base of B3LYP 6-31G*. To our delight the optimized structures for both the anion complexes showed a well cooperative binding motif in which the anion sits above the electron-deficient triazine plane and simultaneously interacts with the two hydroxyl groups and one bromo site from the pendant phenyl group (Figure S47).

Synthesis. In order to quickly access the ransporters **1** and **2**, the straightforward and convenient one-pot strategy was applied (Scheme 1). The dichloro-substituted triazine monomers **3** were facilely prepared through nucleophilic substitution of cyanuric chloride with a series of phenol derivatives containing bromo or iodo

halogen-bonding groups. One-pot reactions between the gallic acid ester derivatized, benzyl protecting diphenol monomers **4** and the triazine monomers **3** in the presence of K_2CO_3 as acid scavenger in refluxed acetonitrile readily afforded the macrocyclic compounds **5** in 41-65% yields. The following deprotection of **5** with an excess amount of $AlCl_3$ in dry toluene proceeded smoothly at ambient temperature and gave transporters **1** in 68-82% yields. For synthesis of transporters **2**, gallic acid ester derived diphenol monomer **9** bearing amide substituent on 4-hydroxy position was firstly prepared by two simple substitution and deprotection steps from **6**. The one-pot reactions between the two monomers **9** and **3** gave transporters **2** in moderate yields. The successful synthesis of **1** and **2** represents a rare example on facile one-pot preparation of functionalized oxacalix[2]arene[2]triazines with considerable yields.

For synthesis of the macocyclic analogue **12** without halogen-bond donor sites, the dichloro-substituted macrocyclic precursor **10** was firstly reacted with two equivalents of phenol in the presence of K_2CO_3 under reflux to give the product **11** in 51% yield (Scheme 2). The following debenzylation with $AlCl_3$ in toluene provided the desired macrocycle **12** in 76% yield. All the compounds were fully characterized with spectroscopic and elemental analyses.

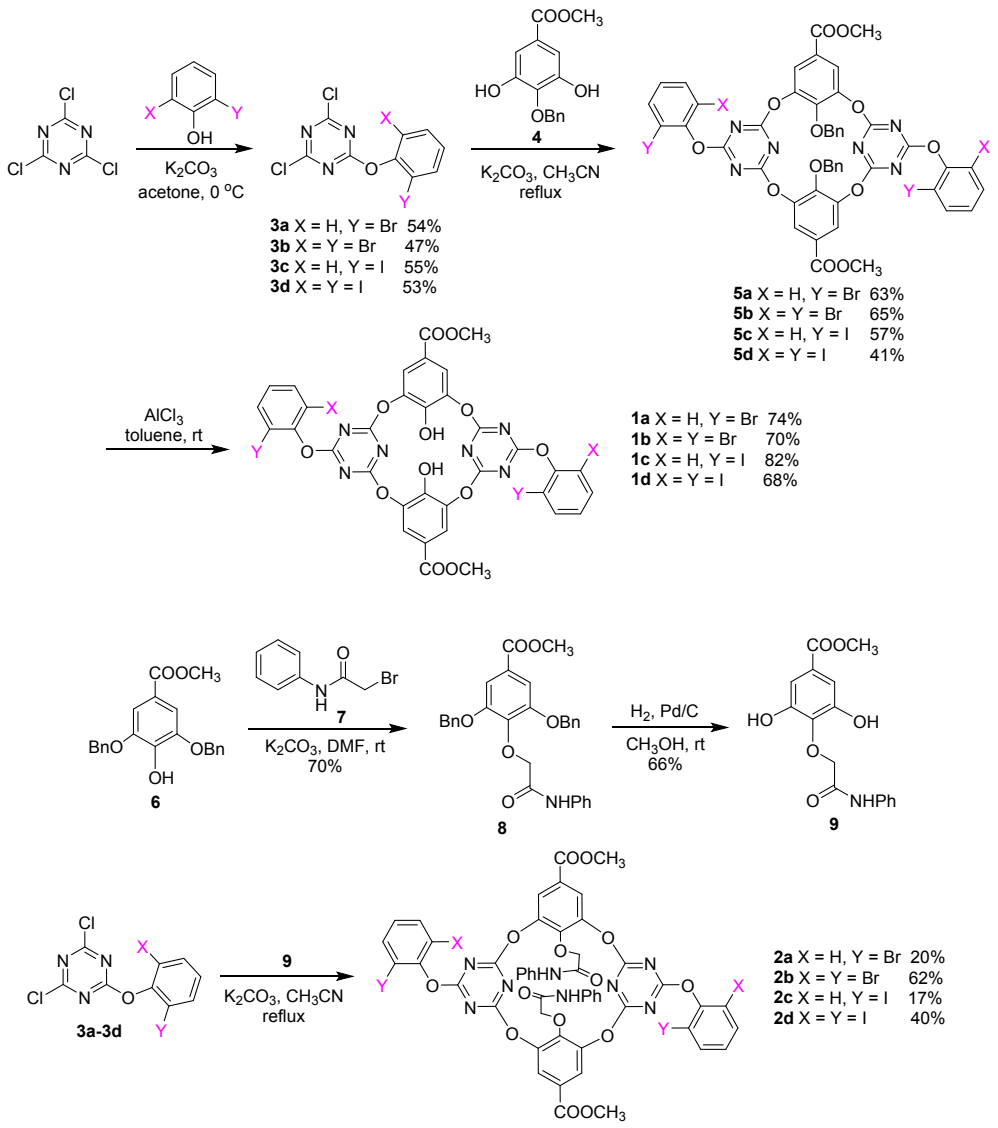

Scheme 1. Synthesis of macrocyclic transporters **1** and **2**.

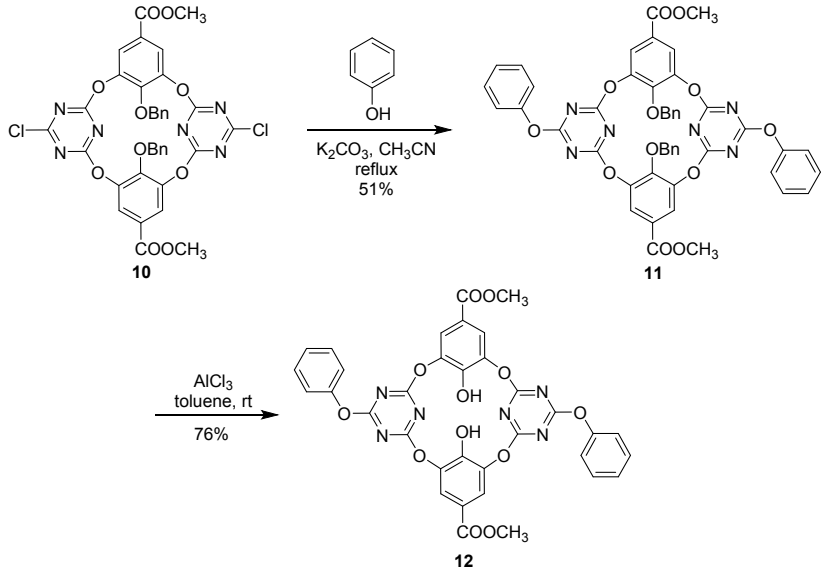

Scheme 2. Synthesis of macrocycle **12** without halogen-bond donor sites.

Anion Binding Studies. The affinity of **1** and **2** towards Cl^- and Br^- (as Bu_4N^+ salts) was assessed by ^1H NMR titrations in d_6-acetone (Figures S3-S28). From the NMR spectra illustrated in Figures S3-S6, treatment of **1** with chloride caused significant downfield shifts of the hydroxyl proton signals, along with slight upfield shifts of the proton signals on the halogen substituted benzene. The downfield shift of hydroxyl proton signal suggests the consistent inclusion of chloride within the electron-deficient V-shape cavity, where the hydroxyl protons co-participate in the anion binding through hydrogen bonding.[17] The upfield shifts of the halogen-substituted benzene proton signals can be attributed to the formation of halogen bonding. Chloride binding with **1** is therefore achieved by a combination of anion-π, hydrogen and halogen bonding. Interaction of **1** with bromide resulted in different chemical shift changes. Besides the general upfield shifts for the halogen-substituted benzene proton signals, the hydroxyl proton signals, however, gradually moved to upfield upon the addition of bromide, which seems strange at first glance. This unusual upfield shift of the hydroxyl signals could reflect a subtle balance between the hydrogen-bonding induction effect and aromatic ring shielding effect. As suggested by the calculation (Figure S47), upon binding the hydroxyl proton was pulled above the triazine ring and shielded by the aromatic plane. In case of bromide, the shielding effect caused upfield shift could be more predominant than hydrogen-bonding induced downfield shift due to its less hydrogen bonding ability than chloride. In contrast, hosts **2** showed similar response to both halides. The significant downfield shifts of amide proton signals and slight upfield shifts of halogen-substituted aryl proton signals suggested consistent halide binding through combination of hydrogen and halogen bonding. The strength of anion binding ($K_{a1:1}$) was calculated by fitting the titration data with *HypNMR 2004* program. The 1:1 binding stoichiometry was further verified by a Job's plot experiment (see Supporting Information). As shown in Table 1, **1** and **2** show strong affinity to halides, giving association constants in the range of 10^2–10^4 M^{-1}, and overall stronger binding

towards chloride than bromide. Moreover, for the two types of transporters, the association constants nearly follow the same order of **a** < **b** < **c** < **d**. As the halogen-bond donor ability follows an order of Cl < Br < I,[8a] the consistent order for the binding affinity further confirms the contribution of halogen bonding.

Table 1. Association Constants ($K_{a1:1}$, M^{-1}) of **1**, **2** with $Bu_4N^+Cl^-$ and $Bu_4N^+Br^-$[a]

	$Bu_4N^+Cl^-$	$Bu_4N^+Br^-$
1a	$(7.37 \pm 0.32) \times 10^3$	$(1.00 \pm 0.06) \times 10^3$
1b	$(9.38 \pm 0.05) \times 10^3$	$(6.86 \pm 0.11) \times 10^2$
1c	$(3.43 \pm 0.46) \times 10^4$	$(1.55 \pm 0.19) \times 10^3$
1d	$(1.30 \pm 0.18) \times 10^4$	$(6.34 \pm 0.18) \times 10^2$
2a	$(6.03 \pm 0.06) \times 10^3$	$(8.97 \pm 0.05) \times 10^2$
2b	$(4.15 \pm 0.27) \times 10^3$	$(5.25 \pm 0.08) \times 10^2$
2c	$(9.00 \pm 0.11) \times 10^3$	$(1.70 \pm 0.14) \times 10^3$
2d	$(4.70 \pm 1.39) \times 10^4$	$(1.04 \pm 1.37) \times 10^4$

[a] Determined by ^1H NMR titrations in d_6-acetone. The association constant was obtained by fitting the titration data with *HypNMR 2004* program.

Crystallographic Studies. To probe the contribution of different types of noncovalent bonds to anion binding from molecular level, single crystals of anion complexes with halides were cultivated. Pleasantly, single crystals of high quality for complexes [**1b**·Cl]$^-$ and [**1c**·Cl]$^-$ were obtained and their structures were determined. As illustrated in Figures 2-3, in both complexes, chloride is included within the electron-deficient cavity formed with triazines through multiple noncovalent interactions including anion-π, hydrogen and halogen bonding. The different interaction details depending on the host structures are worth addressing. In case of [**1b**·Cl]$^-$, a hydrogen bonded Cl5-O14-Cl4 guest triplet is stabilized within the V-shape host cavity. In particular, Cl5 locates above one triazine ring with a short contact ($d_{Cl5\text{-}C20}$ = 3.204 Å), indicating the formation of anion-π interaction.

Moreover, it forms hydrogen bonding with one hydroxyl group ($d_{Cl5\text{-}O10}$ = 2.981 Å) and halogen bonding with one bromine (Br3) on the adjacent macrocycle ($d_{Cl5\text{-}Br3}$ = 3.468 Å). Notably, the distance between Cl5 and neibouring Br1 ($d_{Cl5\text{-}Br1}$ = 3.998 Å) is considerably larger than the sum of their van der Waals radius, suggesting negligible interaction. Such result is most probably due to that the strict directionality of halogen bonding disfavors its intra-cavity cooperation with anion-π and hydrogen bonding. The multiple noncovalent interactions involved with chloride (Cl5) facilitate intermolecular self-assembly to form an extened structure as shown in Figure 2B.

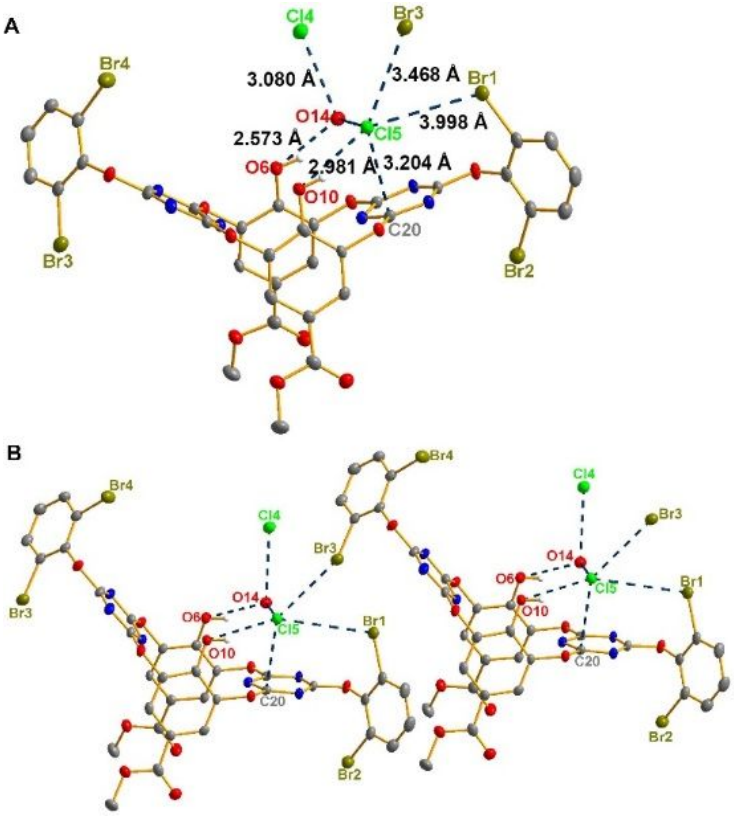

Figure 2. Crystal structure of [**1b**·Cl]$^-$ complex. (A) Participation of noncovalent interactions in chloride binding and (B) intermolecular self-assembly. Countercations and nonessential hydrogen atoms are omitted for clarity. Ellipsoid probability is 25%.

In case of [**1c**·Cl]$^-$, two types of capsule-like structures, namely, **capsule 1** and **capsule 2** as shown in Figure 3A and 3B are observed. In **capsule 1**, two iodine-substituted aryl groups adopt a *syn* orientation on the macrocyclic skeleton and

two of such macrocycle molecules form a semi-cage cavity through intermolecular halogen-bonding between the inward iodines ($d_{I2A\text{-}I1A}$ = 3.906 Å). Chloride (Cl1) is included within the cavity through cooperative anion-π ($d_{Cl1\text{-}plane}$ = 3.086 Å) and duplicate hydrogen bonds ($d_{Cl1\text{-}O6A}$ = 2.943 Å, $d_{Cl1\text{-}O10A}$ = 3.100 Å). Halogen bonding doesn't participate in the binding with chloride as judged from the long distance to the adjacent I2A ($d_{Cl1\text{-}I2A}$ = 4.645 Å). The countercation, Et_4N^+, is included in between the two chlorides to compensate the electrostatic repulsion. In contrast, in **capsule 2**, the two iodines (I1 and I2) are in *anti* orientation and no longer convergent. Besides the similar, cooperative anion-π and hydrogen bonding as observed in **capsule 1**, the chloride (Cl2) also enjoys halogen bonding with I1. These noncovalent interactions direct the formation of a more oblate capsular structure. Notably, the outward iodines (I2) from two adjacent macrocycles form halogen bonding with a "free" chloride (Cl3), leading to one-dimension self-assembly (Figure 3C).

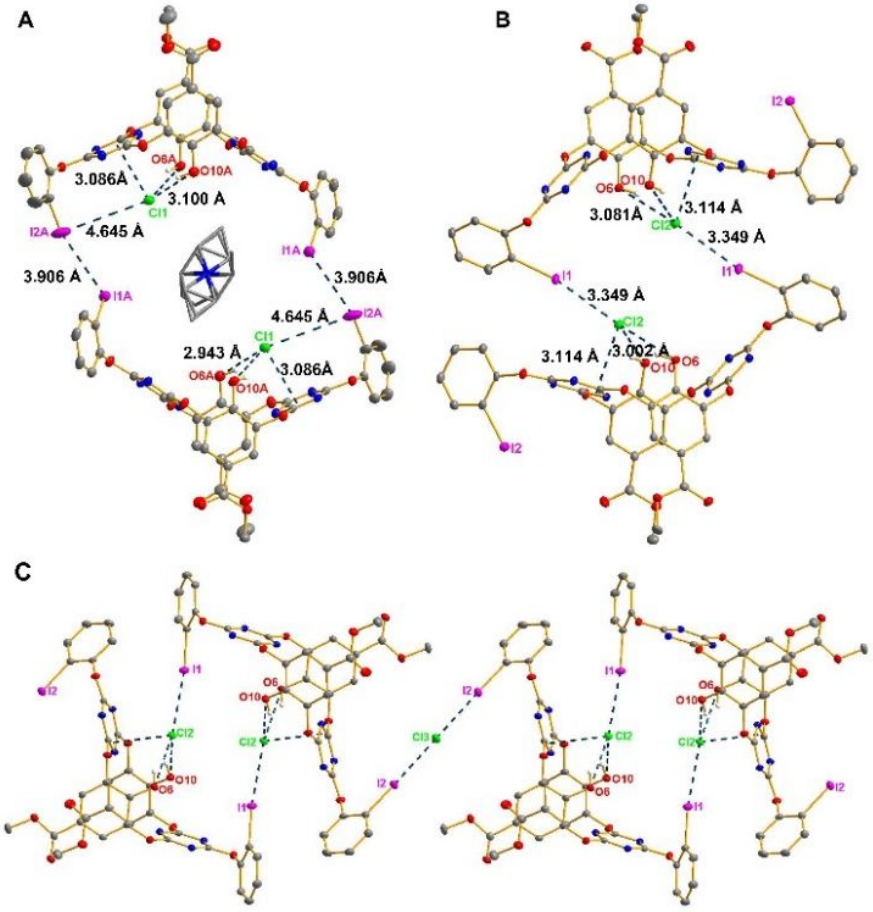

Figure 3. Crystal structure of [**1c**·Cl]$^-$ showing two types of capsular structures. (A)

Capsule 1, (B) **capsule 2**, and (C) intermolecular self-assembly of **capsule 2**. Nonessential countercations and hydrogen atoms are omitted for clarity. Ellipsoid probability is 25%.

Anion Transport Studies. Encouraged by the anion binding study, we then performed a fluorescence assay to evaluate the anion transport activities of **1** and **2**. In this assay, large unilamellar vesicles composed of egg yolk phosphatidylcholine (EYPC LUVs) were loaded with halide selective dye lucigenin as anion transport indicator, then the target transmembrane anion gradient across the membrane was applied. After the addition of transporters, the fluorescent intensity with time was recorded. The fluorescence kinetics of chloride transport in the presence of **1** and **2 (**5 μM) are shown as Figure 4.

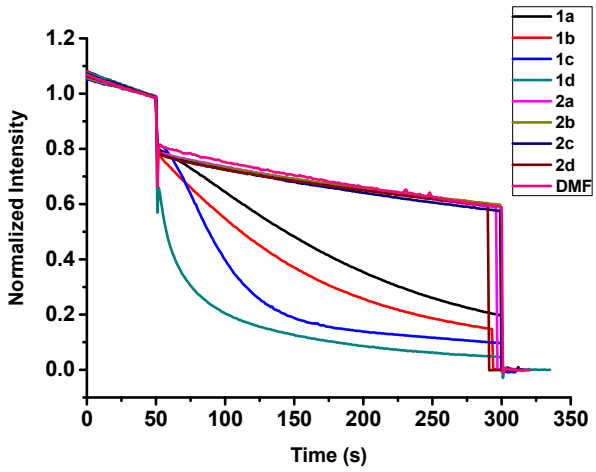

Figure 4. Evaluation of the chloride transport activity of transporters **1** and **2** by lucigenin ⊂ EYPC-LUV fluorescence assays (concentration for each compound is 5 μM).

Surprisingly, although the two series of host compounds bind chloride with comparable affinity, only **1a-d** give significant chloride transport activity. To understand the contrasting transport behaviors of **1** and **2**, we did Hill analyses of the dose-response curve with NaCl as the extravesicular salt for transporters **1a-d**. The effective concentrations (EC_{50}) and Hill coefficients (n) are compiled in Table 2 (for

graph see Figures S30-S33). The EC_{50} values for chloride transport are in the range of 3.1 to 7.4 μM, and suggest an order of transport activity **1d** > **1c** > **1b** > **1a**. Such halogen-bond dependent order indicates the contribution of halogen bonding to chloride transport. When we applied **1a-d** to bromide transport assay, the transporters gave same halogen-bond dependent activities, which further indicates the function of halogen bonding. For contribution of other noncovalent bonds, we applied two structural anlogues to investigate the structure-activity relationship. Removing of the two lower-rim hydroxyl groups and also the ester groups (compound **13**,[18] Figure S29) caused complete inactivation of chloride transport. Alternatively, removing of the halo atoms (compound **12**) showed comparable activity (Table 2, Figure S34) to that of **1d**, which on one hand highlights the contribution of hydroxyl groups, on the other hand suggests the largely reduced thermodynamic chloride binding (K_a = 560 M^{-1}) to **12** could increase the transport activity.[19] The other explanation could be that different "active" strutures are possibly responsible for the transport, *e.g.* a capsular assembly for **1** and a simpler molecular structure for **12**. Taken together, the ion transport is probably mediated by a balance and cooperation of different noncovalent bonds in the molecular backbone. Besides, the obtained Hill coefficients for chloride and bromide are higher than 1 (n > 1), suggesting that halogen-bonded capsule (as shown in Figure 3) may act as the active entity for anion transport. The negligible transport activity of **2a-d** once again suggests the importance of the closely attached low-rim hydroxyl groups.

Table 2. EC_{50} (μM, mol%) and Hill coefficients (n) of **1a-d** with Various Salts.

		LiCl	NaCl	KCl	RbCl	CsCl	NaBr
1a	EC_{50} (μM)	9.4±0.5	7.4±0.5	4.6±0.2	4.0±0.4	4.8±0.2	10.3±1.7
	EC_{50} (mol%)	5.4	4.3	2.7	1.7	2.8	6.0
	n	2.8±0.6	3.2±0.7	7.8±2.0	4.6±2.0	6.5±2.8	3.0±1.7
1b	EC_{50} (μM)	6.6±0.2	5.5±0.1	5.1±0.4	4.0±0.1	4.4±0.2	7.2±0.6
	EC_{50} (mol%)	3.8	3.2	3.0	2.3	2.6	4.2

	n	3.3±0.4	4.1±0.4	4.2±2.2	4.7±0.4	4.5±0.9	3.2±0.9
	EC_{50} (μM)	5.4±0.7	4.0±0.2	3.9±0.1	3.5±0.1	2.9±0.1	7.0±1.1
1c	EC_{50} (mol%)	3.1	2.3	2.3	2.0	1.7	4.1
	n	3.3±1.1	3.2±0.6	2.9±0.9	4.4±0.6	4.5±0.7	2.4±0.9
	EC_{50} (μM)	3.2±0.1	3.1±0.1	2.8±0.1	2.8±0.2	2.7±0.1	2.8±0.1
1d	EC_{50} (mol%)	1.9	1.8	1.6	1.6	1.6	1.6
	n	3.3±0.3	2.2±0.2	3.0±0.3	3.5±0.7	3.0±0.2	3.4±0.3
	EC_{50} (μM)		2.2±0.7				
12	EC_{50} (mol%)	-	1.3	-	-	-	-
	n		1.3±0.7				

To probe the transport mechanism, fluorescence assay with LUVs containing carboxyfluorescein (CF) was performed. Upon the addition of transporters **1a-d**, no fluorescence enhancement was observed, indicating the transporters do not induce the membrane defects (Figure S35). We then set up assays applying vesicles prepared with dipalmitoyl phosphatidylcholine (DPPC), a lipid showing a gel to liquid crystalline transition phase at 41 °C. Transport assay at 25 °C gave dramatically reduced transport activity due to the decrease of membrane fluidity, suggesting that the ion transport process is governed by a carrier mechanism (Figure S37). To investigate whether the transport is through a Cl^-/NO_3^- antiport process, we prepared the vesicles containing lucigenin and sodium chloride. Nitrate and the control anion sulfate were added to the extravesicular buffer solution, respectively. In both cases the intensity of quenched lucigenin was recovered with the release of chloride to the extravesicular buffer, showing independence of chloride efflux on external NO_3^- or SO_4^{2-} (Figure S36). As sulfate is an extremely hydrophilic anion and it is normally impossible to be transported from aqueous solution to the lipid bilayer membrane, the results thus indicate the less possibility of a Cl^-/NO_3^- antiport exchange. The influence of the external cations (alkali metal) on the transport activity was further investigated. As illustrated in Table 2, the transport activities (EC_{50}s) of **1a-d** show cation

dependence. For different cations, the activities follow an overall sequence of $Li^+ < Na^+ < K^+ \approx Rb^+ \approx Cs^+$. These outcomes suggest the ion transport is most probably through an X^-/M^+ ion-pair process. To further shed light on the transport mechanism, i.e. Cl^-/M^+ or Cl^-/NO_3^-, we performed HPTS/FCCP experiment with **1d** chosen as a typical example. According to the results, the activity of **1d** in the presence of FCCP is only a sum of **1d** and FCCP alone, and no additional effect was observed (Figure S38). Besides, we also applied the potassium transporter valinomycin to the lucigenin ⊂ EYPC-LUV system. The coexistence of **1d** and valinomycin showed a similar activity in comparison with **1d** alone (valinomycin alone did not show any significant activity) (Figure S39). Hence both the experiments further supported the Cl^-/M^+ mechanism. The ion pair binding mode could be similar to that observed in crystal structure, i.e. X^- is bound through the multiple noncovalent interactions, where M^+ as countercation sits around and interacts with hydroxyl oxygen atom through ion-dipole interaction.

Evaluation of Anticancer Activities. The efficient transport activity demonstrated by transporters **1** encouraged us to examine their possible application as anticancer chemotherapy agents.[12] The anticancer activity of transporters was evaluated using the colorectal carcinoma cell line HCT116 which were cultured in Dulbecco's Modified Eagle Medium in the presence of KCl with different concentrations of transporters ranging from 0 to 200 μM (Figure 5). For comparison, the anticancer activities of **2c**, **2d** and compound **13** were also investigated. Cell viabilities determined after culturing the cells for 1 day at 37 °C with 5% CO_2 in the presence of transporters **1**, show that HCT116 cells are sensitive to the drugs in a concentration dependent manner. As shown in Figure 5, in the presence of 60 mM KCl, addition of transporters **1** ([**1**] = 200 μM) lead to 11.9 (**1a**), 24.9 (**1b**), 14.9 (**1c**) and 16.0% (**1d**) cell survival, indicating their efficient ability to inhibit tumor cell growth with **1a** being the most potent one. The IC_{50} values calculated are 52.3 μM for **1a**, 58.9 μM for **1b**, 66.4 μM for **1c** and 54.8 μM for **1d**. Not surprisingly, the control compounds **2c**, **2d** and **13** did not show significant effect on the cell growth, suggesting the correlation between transport activity and anticancer activity. We

further determined the cell viabilities at different concentrations of KCl with various concentrations of transporters. All four transporters (**1a**, **1b**, **1c**, **1d**) show good anticancer activities while the control molecules did not (Figures S40-S46).

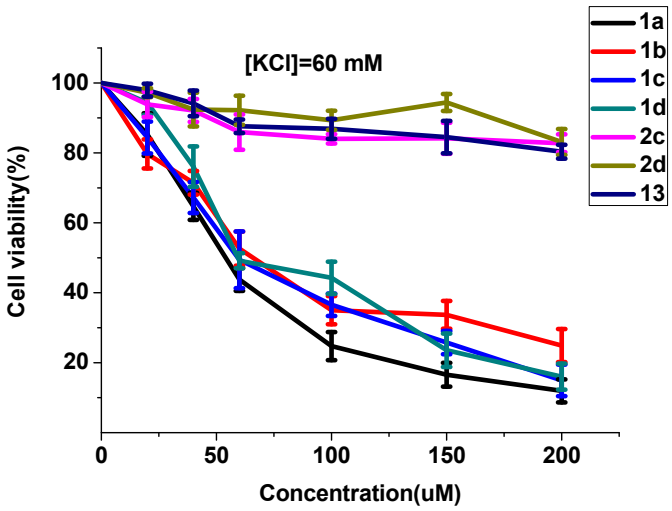

Figure 5. Viabilities of HCT116 cells in the presence of various concentrations of transporters or control compounds at [KCl] = 60 mM.

Conclusions

In conclusion, we have designed oxacalix[2]arene[2]triazine-derived ion transporters **1** and **2** by incorporating multiple noncovalent bonds in close proximity. The manipulation of noncovalent balance was exemplified by anion recognition study in solution and solid state. Both compounds showed strong halide affinity through combination of anion-π, hydrogen and halogen bonding. Fluorescence assays for transmembrane activity distinguished compounds **1** as efficient transporters. Systematic study indicated the ion transport was mediated with a balance of multiple noncovalent bonds including halogen bonding, hydrogen bonding and anion-π interactions. Transporters **1** were revealed to show efficient inhibit of HCT116 cell, which promise their future as potential anticancer chemotherapy agents.

EXPERIMENTAL SECTION

General Information. Reagents for synthesis and analysis were purchased from J&K or Sigma-Aldrich. Egg yolk phosphatidylcholine (EYPC) and a Mini-Extruder used for vesicle preparation were purchased from Avanti Polar Lipids. ^{1}H and ^{13}C NMR spectra were recorded on 300, 400 or 500 MHz spectrometers. Chemical shifts are reported in ppm versus tetramethylsilane with either tetramethylsilane or the residual solvent resonance used as an internal standard. Abbreviations are used in the description of NMR data as follows: chemical shift (δ, ppm), multiplicity (s = singlet, d = doublet, t = triplet, dd = doublet of doublets, m = multiplet), coupling constant (*J*, Hz). Melting points are uncorrected. Infrared spectra were recorded on Nicolet-6700 FT-IR spectrometer. Mass spectra were obtained on BIFLEX Ⅲ, Bruker Inc. (MALDI-TOF) and Bruker APEX-2 (HRMS). Elemental analysis was recorded on Thermo Quest CE Instruments flash EA 1112 analyser. Single crystal X-ray diffraction data were collected on a MM007HF Saturn724+ diffractometer using MoK/α radiation (λ=0.71073 Å or 0.710747 Å) at a temperature of 173 K. All anhydrous solvents were dried according to standard procedures prior to use. All other major chemicals were obtained from commercial sources and used without further purification.

Synthesis Procedures.

General procedure for synthesis of 3. In an ice bath, anhydrous potassium carbonate powder (20 mmol), cyanuric chloride (20 mmol) and acetone (100 mL) were mixed in a flask. The solution of the corresponding phenol derivative (20 mmol) in acetone (100 mL) was then added dropwise within 2 h. The resulting mixture was stirred for 1 h in ice bath condition. After filtration, the filtrate was concentrated and chromatographed on a silica gel column (100-200 mesh). The obtained solid was recrystallized to give pure compound **3** as a white solid.

2,4-dichloro-6-(2-bromophenoxyl)-1,3,5-triazine (3a). Chromatography with a mixture of petroleum ether and acetone (35/1, v/v) and recrystallized from hexane. 54% yield. mp 91-92 ^{o}C; ^{1}H NMR ($CDCl_3$/300 MHz) δ 7.68 (dd, *J* = 1.1, 7.6 Hz, 1H), 7.42 (td, *J* = 1.4, 7.7 Hz, 1H), 7.27-7.21 (m, 2H); $^{13}C\{1H\}$ NMR ($CDCl_3$/75 MHz) δ

173.4, 170.8, 148.6, 134.0, 129.2, 128.6, 123.1, 115.8; IR (KBr) ν 1521, 1403, 1200 cm^{-1}; MS (EI-MS) *m/z* (%): 240 $[M-Br]^+$ (100), 242 $[M-Br]^+$ (50), 244 $[M-Br]^+$ (10). Anal. Calcd. for $C_9H_4BrCl_2N_3O$: C, 33.68; H, 1.26; N, 13.09. Found: C, 33.72; H, 1.26; N, 12.98.

2,4-dichloro-6-(2,6-dibromophenoxyl)-1,3,5-triazine (3b). Chromatography with a mixture of petroleum ether and acetone (30/1, v/v) and recrystallized from hexane. 47% yield. mp 136-137 °C; ^1H NMR ($CDCl_3$/300 MHz) δ 7.63 (d, J = 8.1 Hz, 2H), 7.12 (t, J = 7.8, 8.1 Hz, 1H); $^{13}C\{1H\}$ NMR ($CDCl_3$/75 MHz) δ 173.5, 170.0, 146.2, 133.0, 129.2, 117.2; IR (KBr) ν 1521, 1394, 1211 cm^{-1}; MS (EI-MS) *m/z* (%): 318 $[M-Br]^+$ (50), 320 $[M-Br]^+$ (100), 322 $[M-Br]^+$ (35), 324 $[M-Br]^+$ (5). Anal. Calcd. for $C_9H_3Br_2Cl_2N_3O$: C, 27.03; H, 0.76; N, 10.51. Found: C, 27.10; H, 0.80; N, 10.57.

2,4-dichloro-6-(2-iodophenoxyl)-1,3,5-triazine (3c). Chromatography with a mixture of petroleum ether and acetone (30/1, v/v) and recrystallized from hexane and acetone. 55% yield. mp 97-98 °C; ^1H NMR ($CDCl_3$/300 MHz) δ 7.90 (dd, J = 1.2, 6.0 Hz, 1H), 7.45 (td, J = 1.2, 6.0 Hz, 1H), 7.18 (dd, J = 1.2, 6.0 Hz, 1H), 7.09 (td, J = 1.2, 6.0 Hz, 1H); $^{13}C\{1H\}$ NMR ($CDCl_3$/75 MHz) δ 173.3, 170.7, 151.5, 140.1, 130.1, 128.8, 122.5, 89.4; IR (KBr) ν 1527, 1402, 1193 cm^{-1}; MS (EI-MS) *m/z* (%): 240 $[M-I]^+$ (100), 242 $[M-I]^+$ (50), 244 $[M-I]^+$ (10). Anal. Calcd. for $C_9H_4Cl_2IN_3O$: C, 29.38; H, 1.10; N, 11.42. Found: C, 29.31; H, 1.16; N, 11.47.

2,4-dichloro-6-(2,6-diiodophenoxyl)-1,3,5-triazine (3d). Chromatography with a mixture of petroleum ether and acetone (30/1, v/v) and recrystallized from hexane and acetone. 53% yield. mp 150-151 °C; ^1H NMR ($CDCl_3$/300 MHz) δ 7.86 (d, J = 7.9 Hz, 2H), 6.80 (t, J = 7.9 Hz, 1H); $^{13}C\{1H\}$ NMR ($CDCl_3$/75 MHz) δ 173.5, 169.9, 151.3, 140.1, 130.1, 89.6; IR (KBr) ν 1523, 1394, 1206 cm^{-1}; MS (CI-MS) *m/z* (%): 365.8 $[M-I]^+$ (100), 367.8 $[M-I]^+$ (67), 369.8 $[M-I]^+$ (15). Anal. Calcd. for $C_9H_3Cl_2I_2N_3O$: C, 21.89; H, 0.61; N, 8.51. Found: C, 21.94; H, 0.78; N, 8.54.

General procedure for synthesis of 5. Fine anhydrous potassium carbonate powder (10 mmol) and acetonitrile (100 mL) were mixed in a flask and heated at reflux. The solution of **4** (4 mmol) and **3** (4 mmol) in acetonitrile (100 mL) was then added dropwise within 2 h. The resulting mixture was refluxed for another 10 min and

cooled to room temperature. After filtration, the filtrate was concentrated and chromatographed on a silica gel column (100-200 mesh) to give pure compound **5** as a white solid.

5a. Chromatography with a mixture of petroleum ether, chloroform and acetone (10/2/1, v/v/v). 63% yield. mp 174-175 ^{o}C; ^{1}H NMR ($CDCl_3$/300 MHz) δ 7.65 (d, J = 8.1 Hz, 2H), 7.59 (s, 4H), 7.40 (t, J = 7.5 Hz, 2H), 7.23-7.06 (m, 14H), 4.88 (s, 4H), 3.85 (s, 6H); ^{13}C{1H} NMR ($CDCl_3$/75 MHz) δ 173.7, 173.1, 164.8, 149.0, 146.5, 144.8, 135.6, 133.6, 128.9, 128.3, 128.2, 127.9, 127.7, 125.7, 123.4, 122.0, 116.2, 75.3, 52.4; IR (KBr) ν 1729, 1568, 1368, 1211 cm^{-1}; MS (MALDI-TOF) *m/z* (%): 1065.0 $[M+Na]^+$ (20), 1067.0 $[M+Na]^+$ (100), 1069.1 $[M+Na]^+$ (40). Anal. Calcd. for $C_{48}H_{32}Br_2N_6O_{12}$: C, 55.19; H, 3.09; N, 8.05. Found: C, 55.04; H, 3.32; N, 7.92.

5b. Chromatography with a mixture of petroleum ether, chloroform and acetone (10/3/1, v/v/v). 65% yield. mp >300 ^{o}C; ^{1}H NMR ($CDCl_3$/300 MHz) δ 7.61-7.29 (m, 8H), 7.18-7.06 (m, 12H), 4.86 (s, 4H), 3.86 (s, 6H); ^{13}C{1H} NMR ($CDCl_3$/75 MHz) δ 173.2, 173.0, 165.0, 146.8, 146.5, 145.0, 135.6, 132.8, 128.7, 128.5, 128.3, 128.0, 125.9, 122.2, 117.8, 75.4, 52.6; IR (KBr) ν 1730, 1562, 1360, 1224 cm^{-1}; MS (MALDI-TOF) *m/z* (%): 1224.8 $[M+Na]^+$ (100), 1226.8 $[M+Na]^+$ (60). Anal. Calcd. for $C_{48}H_{30}Br_4N_6O_{12}$: C, 47.95; H, 2.51; N, 6.99. Found: C, 47.92; H, 2.59; N, 7.12.

5c. Chromatography with a mixture of petroleum ether, chloroform and acetone (9/2/1, v/v/v). 57% yield. mp 224-225 ^{o}C; ^{1}H NMR ($CDCl_3$/300 MHz) δ 7.86 (dd, J = 1.5, 6.6 Hz, 2H), 7.59 (s, 4H), 7.41 (td, J = 1.5, 6.6Hz, 2H), 7.23-7.02 (m, 14H), 4.93 (s, 4H), 3.86 (s, 6H); ^{13}C{1H} NMR ($CDCl_3$/75 MHz) δ 173.7, 173.2, 164.9, 152.1, 146.6, 145.0, 139.9, 135.8, 129.9, 128.5, 128.3, 128.2, 127.8, 125.8, 122.8, 122.1, 90.3,75.4, 52.6; IR (KBr) ν 1728, 1567, 1367, 1207 cm^{-1}; MS (MALDI-TOF) *m/z* (%): 1011.1 $[M-I]^+$ (100), 1139.0 $[M+H]^+$ (25), 1161.0 $[M+Na]^+$ (35). Anal. Calcd. for $C_{48}H_{32}I_2N_6O_{12}$: C, 50.63; H, 2.83; N, 7.38. Found: C, 50.47; H, 2.94; N, 7.33.

5d. Chromatography with a mixture of petroleum ether, chloroform and acetone (5/1/0.4, v/v/v). 41% yield. mp 282-283 ^{o}C; ^{1}H NMR ($CDCl_3$/300 MHz) δ 7.81 (d, J = 7.8 Hz, 4H), 7.64 (s, 4H), 7.18-7.08 (m, 10H), 6.74 (t, J = 7.9 Hz, 2H), 4.96 (s, 4H), 3.86 (s, 6H); ^{13}C{1H} NMR ($CDCl_3$/75 MHz) δ 173.2, 172.8, 164.8, 151.8, 146.5,

144.9, 139.8, 135.9,129.6, 128.6, 128.1, 127.8, 125.9, 122.2, 90.3, 75.2, 52.6; IR (KBr) ν 1731, 1571, 1356, 1216 cm^{-1}; MS (MALDI-TOF) *m/z* (%): 1412.3 $[M+Na]^+$ (100). Anal. Calcd. for $C_{48}H_{30}I_4N_6O_{12}$: C, 41.46; H, 2.17; N, 6.04. Found: C, 41.48; H, 2.22; N, 5.96.

General procedure for synthesis of 1. At room temperature, **5** (0.25 mmol), anhydrous aluminum chloride (7.5 mmol) and dried toluene (20 mL) were mixed in a flask. The mixture was stirred for 5 h under argon gas and poured into ice water (20 mL), then extracted with ethyl acetate (2×20 mL). The organic phase was dried with anhydrous sodium sulfate and filtered. After removal of organic solvent, the residue was recrystallized with ethyl acetate to give pure compound **1** as a white solid.

1a. 74% yield. mp 239-240 °C; ^{1}H NMR (d_6-acetone/300 MHz) δ 7.79 (dd, *J* = 1.5, 8.0 Hz, 2H), 7.55 (td, *J* =1.5, 8.2 Hz, 2H), 7.48 (s, 4H), 7.45 (dd, *J* =1.6, 8.1 Hz, 2H), 7.33 (td, *J* =1.6, 8.1 Hz, 2H), 3.79 (s, 6H); ^{13}C{1H} NMR (d_6-acetone/75 MHz) δ 174.8, 174.5, 165.4, 150.2, 147.2, 141.2, 134.5, 130.0, 129.0, 124.9, 122.7, 121.7, 116.5, 52.4; IR (KBr) ν 3164, 1731, 1568, 1366, 1213 cm^{-1}; MS (ESI) *m/z* (%): 861.3 $[M]^-$ (80), 863.3 $[M]^-$ (100), 865.3 $[M]^-$ (75). HRMS (ESI): *m/z* calcd. for $[M+H]^+$ $C_{34}H_{21}Br_2N_6O_{12}$: 862.9579; found 862.9562.

1b. 70% yield. mp 262-263 °C; ^{1}H NMR (d_6-acetone/300 MHz) δ 7.81 (d, *J* = 8.1 Hz, 4H), 7.50 (s, 4H), 7.30 (t, *J* =8.1 Hz, 2H), 3.79 (s, 6H); ^{13}C{1H} NMR (d_6-DMSO/75 MHz) δ 173.0, 172.1, 164.4, 146.4, 145.9, 140.1, 133.0, 129.5, 121.8, 119.2, 117.1, 51.9; IR (KBr) ν 3445, 1720, 1576, 1363, 1223 cm^{-1}; MS (MALDI-TOF) *m/z* (%): 1045.0 $[M+Na]^+$ (100), 1047.0 $[M+Na]^+$ (50). HRMS (ESI): *m/z* calcd. for $[M+H]^+$ $C_{34}H_{19}Br_4N_6O_{12}$: 1018.7789. Found: 1018.7770.

1c. 82% yield. mp >300 °C; ^{1}H NMR (d_6-acetone/300 MHz) δ 8.10 (dd, *J* = 1.2, 6.6 Hz, 2H), 7.56 (td, *J* =1.2, 6.6 Hz, 2H), 7.48 (s, 4H), 7.39 (dd, *J* =1.2, 6.6 Hz, 2H), 7.18 (td, *J* =1.2, 6.6 Hz, 2H), 3.79 (s, 6H); ^{13}C{1H} NMR (d_6-DMSO/75 MHz) δ 173.1, 172.9, 164.4, 151.6, 146.6, 140.1, 139.4, 129.9, 128.3, 123.3, 121.7, 119.2, 90.8, 51.9; IR (KBr) ν 3396, 1724, 1570, 1367, 1209 cm^{-1}; MS (ESI-MS) *m/z* (%): 957.3 $[M]^-$ (100). Anal. Calcd. for $C_{34}H_{20}I_2N_6O_{12}$: C, 42.61; H, 2.10; N, 8.77. Found: C, 42.73; H, 2.24; N, 8.95.

1d. 68% yield. mp >300 °C; ^{1}H NMR (d_6-acetone/300 MHz) δ 8.02 (d, J = 7.9 Hz, 4H), 7.49 (s, 4H), 6.93 (t, J =7.9 Hz, 2H), 3.80 (s, 6H); ^{13}C{1H} NMR (d_6-acetone/75 MHz) δ 174.6, 174.0, 165.4, 153.0, 147.2, 141.5, 141.0, 130.7, 122.7, 121.8, 91.1, 52.4; IR (KBr) ν 3203, 1724, 1575, 1358, 1217 cm^{-1}; MS (MALDI-TOF) *m/z* (%): 1210.4 $[M+H]^+$ (20), 1232.3 $[M+Na]^+$ (100). HRMS (ESI): *m/z* calcd. for $[M+H]^+$ $C_{34}H_{19}I_4N_6O_{12}$: 1210.7234. Found: 1210.7207.

Synthesis of methyl 3,5-bis(benzyloxy)-4-(2-oxo-2-(phenylamino)ethoxy)benzoate (8). At room temperature, anhydrous potassium carbonate powder (332 mg, 2.4 mmol), **6** (729 mg, 2 mmol) and DMF (10 mL) were added to a flask and stirred for 1 h. Then **7** (2.2 mmol, 471 mg) was added and the reaction mixture was stirred for another 0.5 h. To the mixture was added water (20 mL), and 10% dilute hydrochloric acid to adjust pH = 7. After extracted with ethyl acetate, the organic phase was dried with anhydrous sodium sulfate and filtered. The filtrate was concentrated and chromatographed on a silica gel column (100-200 mesh) with a mixture of petroleum ether and ethyl acetate (6/1, v/v) as an eluent. The obtained solid was recrystallized with petroleum ether and ethyl acetate to give pure compound **8** as a colorless solid (770 mg, 70%). **8:** mp 111-112 °C; ^{1}H NMR (d_6-acetone/300 MHz) δ 9.26 (s, 1H), 7.60-7.57 (m, 4H), 7.52 (s, 2H), 7.43-7.30 (m, 8H), 7.19 (m, 2H), 7.03 (m, 1H), 5.32 (s, 4H), 4.68 (s, 2H), 3.87 (s, 3H); ^{13}C{1H} NMR (d_6-acetone/75 MHz) δ 167.7, 166.6, 152.4, 142.3, 138.9, 137.5, 129.5, 129.1, 128.9, 126.9, 124.6, 120.3, 109.4, 73.4, 72.1, 52.6; IR (KBr) ν 3365, 1716, 1692, 1110 cm^{-1}; MS (EI-MS) *m/z* 406 $[M-Bn]^+$ (100%), 497 $[M]^+$ (9). Anal. Calcd. for $C_{30}H_{27}NO_6$: C, 72.42; H, 5.47; N, 2.82. Found: C, 72.25; H, 5.55; N,2.94.

Synthesis of methyl 3,5-dihydroxy-4-(2-oxo-2-(phenylamino)ethoxy)benzoate (9). Under ice bath, **8** (498 mg, 1 mmol), 10% Pd/C (110 mg), methanol (10 mL) were added to a flask and placed under H_2. The reaction mixture was stirred for 4 h at room temperature. After filtration, the filtrate was concentrated and chromatographed on a silica gel column (100-200 mesh) with a mixture of petroleum ether and acetone (4/1, v/v) as an eluent

to give pure compound **9** as a white solid (210 mg, 66%). **9:** mp 199-200 °C; ^{1}H NMR (d_6-acetone/300 MHz) δ 9.60 (s, 1H), 9.23 (s, 2H), 7.68 (d, J = 7.5Hz, 2H), 7.35 (t, J = 7.5Hz, 2H), 7.13 (t, J = 7.5Hz, 1H), 7.11 (s, 2H), 4.82 (s, 2H), 3.82 (s, 3H); ^{13}C{1H} NMR (d_6-acetone/75 MHz) δ 170.5, 166.8, 151.5, 140.2, 139.0, 129.8, 127.6, 125.1, 120.6, 120.5, 110.1, 72.8, 52.3; IR (KBr) ν 3419 3330, 1706, 1601 cm^{-1}; MS (EI-MS) *m/z* 224 [M-PhNH$_2$-H]$^+$ (100%), 317 [M]$^+$ (5); Anal. Calcd. for $C_{16}H_{15}NO_6$: C, 60.57; H, 4.77; N, 4.41. Found: C, 60.59; H, 4.95; N, 4.26.

General procedure for synthesis of 2. Fine anhydrous potassium carbonate powder (2 mmol) and acetonitrile (40 mL) were mixed in a flask and heated at reflux. The suspension of **6** (0.4 mmol) and **3** (0.4 mmol) in acetonitrile (40 mL) was then added. The resulting mixture was refluxed for another 15 min and cooled to room temperature. After filtration, the filtrate was concentrated and chromatographed on a silica gel column (100-200 mesh) and followed by recrystallization if necessary to give pure compound **2** as a white solid.

2a. Chromatography with a mixture of petroleum ether, chloroform and acetone (7/6/1, v/v/v) and recrystallized from hexane and acetone. 20% yield. mp 263-264 °C; ^{1}H NMR (d_6-acetone/300 MHz) δ 9.01 (s, 2H), 7.72 (dd, J = 3.2, 7.9 Hz, 2H), 7.63-7.61 (m, 8H), 7.39-7.25 (m, 8H), 7.13-7.07 (m, 4H), 4.62 (s, 4H), 3.85 (s, 6H); ^{13}C{1H} NMR (d_6-acetone/75 MHz) δ 175.1, 174.5, 166.2, 166.1, 164.9, 150.0, 147.6, 145.4, 138.9, 138.8, 134.4, 130.0, 129.6, 128.9, 127.0, 125.0, 124.7, 123.5, 120.9, 120.8, 116.4, 73.2, 52.8; IR (KBr) ν 3400, 1729, 1566, 1362, 1212 cm^{-1}; MS (MALDI-TOF) *m/z* (%): 1151.2 [M+Na]$^+$ (45), 1153.2 [M+Na]$^+$ (100), 1155.2 [M+Na]$^+$ (55). Anal. Calcd. for $C_{50}H_{34}Br_2N_8O_{14}$: C, 53.11; H, 3.03; N, 9.91. Found: C, 53.26; H, 3.10; N, 9.83.

2b. Chromatography with a mixture of petroleum ether, chloroform and acetone (8/6/1, v/v/v). 62% yield. mp >300°C; ^{1}H NMR ($CDCl_3$/300 MHz) δ 8.27 (s, 2H), 7.70 (s, 4H), 7.54-7.51 (m, 8H), 7.23 (t, J = 7.8 Hz, 4H), 7.08 (q, J = 8.1 Hz, 4H), 4.56 (s, 4H), 3.90 (s, 6H); ^{13}C{1H} NMR ($CDCl_3$/75 MHz) δ 173.5, 173.5, 164.7, 164.3, 146.5, 145.7, 144.1, 136.7, 132.9, 129.3, 129.0, 127.2, 125.1, 123.2, 120.3, 117.4, 72.8, 52.9; IR (KBr) ν 3405, 3279, 1732, 1564, 1360, 1224 cm^{-1}; MS

(MALDI-TOF) *m/z* (%): 1308.8 $[M+Na]^+$ (60), 1310.8 $[M+Na]^+$ (100), 1312.9 $[M+Na]^+$ (70). Anal. Calcd. for $C_{50}H_{32}Br_4N_8O_{14}$: C, 46.61; H, 2.50; N, 8.70. Found: C, 46.52; H, 2.52; N, 8.55.

2c. Chromatography with a mixture of petroleum ether, chloroform and acetone (7/6/1, v/v/v). 17% yield. mp 184-185 °C; ^{1}H NMR (d_6-acetone /300 MHz) δ 9.03 (s, 2H), 7.93 (dd, *J* = 3.1, 7.9 Hz, 2H), 7.64-7.61 (m, 8H), 7.39-7.25 (m, 6H), 7.14-7.03 (m, 6H), 4.63 (s, 4H), 3.85 (s, 6H); ^{13}C{1H} NMR (d_6-acetone/75 MHz) δ 175.1, 174.5, 166.2, 166.1, 164.9, 153.1, 147.6, 145.5, 140.6, 138.9, 138.8, 130.8, 129.6, 129.0, 127.1, 125.0, 123.9, 123.5, 121.0, 120.9, 90.4, 73.2, 52.8; IR (KBr) ν 3479, 1727, 1566, 1365, 1203 cm^{-1}; MS (MALDI-TOF) *m/z* (%): 1247.1 $[M+Na]^+$ (100), 1249.1 $[M+Na]^+$ (12). Anal. Calcd. for $C_{50}H_{34}I_2N_8O_{14}$: C, 49.04; H, 2.80; N, 9.15. Found: C, 48.93; H, 2.91; N, 8.93.

2d. Chromatography with a mixture of petroleum ether, chloroform and acetone (8/6/1, v/v/v) and recrystallized from cyclohexane and dichloromethane. 40% yield. mp 294-295 °C; ^{1}H NMR (d_6-acetone/300 MHz) δ 8.95 (s, 2H), 7.93 (br, 4H), 7.67 (s, 4H), 7.62 (d, *J* = 7.8 Hz, 4H), 7.24 (t, *J* = 7.8 Hz, 4H), 7.08 (t, *J* = 7.3 Hz, 2H), 6.90 (t, *J* = 7.9 Hz, 2H), 4.64 (s, 4H), 3.85 (s, 6H); ^{13}C{1H} NMR (d_6-acetone/125 MHz) δ 174.5, 174.1, 165.7, 164.9, 152.8, 147.1, 145.4, 140.9, 138.8, 130.8, 129.7, 127.2, 125.0, 123.5, 121.0, 90.9, 73.1, 52.8; IR (KBr) ν 3300, 1730, 1571, 1356, 1215 cm^{-1}; MS (MALDI-TOF) *m/z* (%): 1498.9 $[M+Na]^+$ (100), 1499.9 $[M+Na]^+$ (47). Anal. Calcd. for $C_{50}H_{32}I_4N_8O_{14}$: C, 40.67; H, 2.18; N, 7.59. Found: C, 40.71; H, 2.31; N, 7.49.

Synthesis of 11. Fine anhydrous potassium carbonate powder (154 mg, 1.1 mmol), phenol (105 mg, 1.1 mmol) and acetonitrile (25 mL) were mixed in a flask and heated at reflux for 30 mins. The suspension of **10** (0.386 g, 0.5 mmol) in acetonitrile (45 mL) was then added dropwise within 35 mins. The resulting mixture was refluxed for another 35 mins and cooled to room temperature. After filtration, the filtrate was concentrated and chromatographed on a silica gel column (100-200 mesh) with a mixture of petroleum ether and ethyl acetate (3/1, v/v) as an eluent to give pure compound **11** as a white solid (228 mg, 51%). **11:** mp 113-114 °C; ^{1}H NMR

($CDCl_3$/500 MHz) δ 7.56 (s, 4H), 7.44 (t, *J* = 7.9 Hz, 4H), 7.31 (t, *J* = 7.4 Hz, 2H), 7.23 (t, *J* = 7.4 Hz, 2H), 7.16 (t, *J* = 7.6 Hz, 4H), 7.12 (d, *J* = 7.8 Hz, 4H), 7.07 (d, *J* = 7.5 Hz, 4H), 4.91 (s, 4H), 3.85 (s, 6H); $^{13}C\{^1H\}$ NMR ($CDCl_3$/125 MHz) δ 174.3, 173.2, 165.0, 151.7, 146.8, 145.0, 135.9, 129.8, 128.4, 128.3, 127.6, 126.5, 125.8, 122.2, 121.5, 75.6, 52.6; IR (KBr) ν 1727, 1598, 1362, 1200 cm^{-1}; HRMS (ESI): *m/z* calcd. for $[M+H]^+$ $C_{48}H_{35}N_6O_{12}$: 887.2307; found 887.2287.

Synthesis of 12. At room temperature, **11** (355 mg, 0.4 mmol), anhydrous aluminum chloride (1.092 g, 8 mmol) and dried toluene (40 mL) were mixed in a flask. The mixture was stirred for 3.5 h under argon gas and poured into ice water (50 mL), then extracted with ethyl acetate (2×40 mL). The organic phase was dried with anhydrous sodium sulfate and filtered. After removal of organic solvent, the residue was recrystallized with dichloromethane and hexane to give pure compound **12** as a white solid (215 mg, 76%). **12:** mp 224-225 °C; ^1H NMR (d_6-acetone/500 MHz) δ 9.66 (s, 1H), 7.52 (t, *J* =1.5, 7.8 Hz, 4H), 7.47 (s, 4H), 7.35 (t, *J* =7.5 Hz, 2H), 7.32 (d, *J* =7.7 Hz, 4H), 3.78 (s, 6H); $^{13}C\{^1H\}$ NMR (d_6-acetone/125 MHz) δ 175.4, 174.4, 165.4, 152.9, 147.2, 141.2, 130.6, 127.1, 122.7, 122.5, 121.7, 52.4; IR (KBr) ν 3324, 1721, 1568, 1368, 1199 cm^{-1}; HRMS (ESI): *m/z* calcd. for $[M-H]^-$ $C_{34}H_{21}N_6O_{12}$: 705.1223; found 705.1218.

ASSOCIATED CONTENT

AUTHOR INFORMATION

Corresponding Author

qiqiangw@iccas.ac.cn; dxwang@iccas.ac.cn

Notes

The authors declare no competing financial interests.

ACKNOWLEDGMENTS

This work was financially supported by NNSFC (21772203, 21761132024, 21502200, 21521002), Chinese Academy of Sciences (QYZDJ-SSW-SLH023) and the Project for Extramural Scientists of the State Key Laboratory of Agrobiotechnology (grant 2018SKLAB6-8). Q.-Q.W. also thanks the Thousand Young Talents Program for support.

Supporting Information. Experimental details for binding studies, evaluation of ion transport activity and anticancer activity. Copies of ^{1}H and ^{13}C NMR spectra, and crystallographic data. CCDC 1892121 and 1892122 contain the supplementary crystallographic data for this paper. This material is available free of charge via the Internet at http://pubs.acs.org.

References

1. Davis, J. T.; Okunola, O.; Quesada, R. Recent Advances in the Transmembrane Transport of Anions. *Chem. Soc. Rev.* **2010**, *39*, 3843-3862.
2. (a) Riccardis, F. de; Izzo, I.; Montesarchio, D.; Tecilla, P. Ion Transport through Lipid Bilayers by Synthetic Ionophores: Modulation of Activity and Selectivity. *Acc. Chem. Res.* **2013**, *46*, 2781-2790. (b) Sisson, A. L.; Shah, M. R.; Bhosale, S.; Matile, S. Synthetic Ion Channels and Pores (2004–2005). *Chem. Soc. Rev.* **2006**, *35*, 1269-1286. (c) Davis, A. P.; Sheppard, D. N.; Smith, B. D. Development of Synthetic Membrane Transporters for Anions. *Chem. Soc. Rev.* **2007**, *36*, 348-357. (d) Matile, S.; Jentzsch, A. V.; Montenegro, J.; Fin, A. Recent Synthetic Transport Systems. *Chem. Soc. Rev.* **2011**, *40*, 2453-2474. (e) Valkenier, H.; Davis, A. P. Making a Match for Valinomycin: Steroidal Scaffolds in the Design of Electroneutral, Electrogenic Anion Carriers. *Acc. Chem. Res.* **2013**, *46*, 2898-2909. (f) Gale, P. A.; Davis, J. T.; Quesada, R. Anion Transport and Supramolecular Medicinal Chemistry. *Chem. Soc. Rev.* **2017**, *46*, 2497-2519. (g) Gokel, G. W.; Negin, S. Synthetic Ion Channels: From Pores to Biological Applications. *Acc. Chem. Res.* **2013**, *46*, 2824-2833. (h) Gong, B.; Shao, Z. Self-Assembling Organic Nanotubes with Precisely Defined, Sub-nanometer

Pores: Formation and Mass Transport Characteristics. *Acc. Chem. Res.* **2013**, *46*, 2856-2866. (i) Si, W.; Xin, P.; Li, Z.-T.; Hou, J.-L. Tubular Unimolecular Transmembrane Channels: Construction Strategy and Transport Activities. *Acc. Chem. Res.* **2015**, *48*, 1612-1619. (j) Fyles, T. M. Synthetic Ion Channels in Bilayer Membranes. *Chem. Soc. Rev.* **2007**, *36*, 335-347. (k) Li, X.; Wu, Y.-D.; Yang, D. α-Aminoxy Acids: New Possibilities from Foldamers to Anion Receptors and Channels. *Acc. Chem. Res.* **2008**, *41*, 1428-1438. (l) Huo, Y.; Zeng, H. "Sticky"-Ends-Guided Creation of Functional Hollow Nanopores for Guest Encapsulation and Water Transport. *Acc. Chem. Res.* **2016**, *49*, 922-930. (m) Barboiu, M. Encapsulation versus Self-Aggregation toward Highly Selective Artificial K^+ Channels. *Acc. Chem. Res.* **2018**, *51*, 2711-2718. (n) Gokel, G. W.; Mukhopadhyay, A. Synthetic Models of Cation-conducting Channels. *Chem. Soc. Rev.* **2001**, *30*, 274-286.

3. (a) Seganish, J. L.; Davis, J. T. Prodigiosin is a Chloride Carrier that can Function as an Anion Exchanger. *Chem. Commun.* **2005**, 5781-5783. (b) Gale, P. A.; Light, M. E.; McNally, B.; Navakhun, K.; Sliwinski, K. E.; Smith, B. D. Co-transport of H^+/Cl^- by a Synthetic Prodigiosin Mimic. *Chem. Commun.* **2005**, 3773-3775. (c) Sessler, J. L.; Eller, L R.; Cho, W.-S.; Nicolaou, S.; Aguilar, A.; Lee, J. T.; Lynch, V. M.; Magda, D. J. Synthesis, Anion-Binding Properties, and in Vitro Anticancer Activity of Prodigiosin Analogues. *Angew. Chem. Int. Ed.* **2005**, *44*, 5989-5992.
4. (a) Shank, L. P.; Broughman, J. R.; Takeguchi, W.; Cook, G.; Robbins, A. S.; Hahn, L.; Radke, G.; Iwamoto, T.; Schultz, B. D.; Tomich, J. M. Redesigning Channel-Forming Peptides: Amino Acid Substitutions that Enhance Rates of Supramolecular Self-Assembly and Raise Ion Transport Activity. *Biophys. J.* **2006**, *90*, 2138-2150. (b) Schlesinger, P. H.; Ferdani, R.; Liu, J.; Pajewska, J.; Pajewski, R.; Saito, M.; Shabany, H.; Gokel, G. W. SCMTR: A Chloride-Selective, Membrane-Anchored Peptide Channel that Exhibits Voltage Gating. *J. Am. Chem. Soc.* **2002**, *124*, 1848-1849.
5. Davis, A. P. Anion Binding and Transport by Steroid-based Receptors. *Coord.*

Chem. Rev. **2006**, *250*, 2939-2951.

6. Sakai, N.; Mareda, J.; Matile, S. Rigid-Rod Molecules in Biomembrane Models: From Hydrogen-Bonded Chains to Synthetic Multifunctional Pores. *Acc. Chem. Res.* **2005**, *38*, 79-87.
7. (a) Sidorov, V.; Kotch, F. W.; Abdrakhmanova, G.; Mizani, R.; Fettinger, J. C.; Davis, J. T. Ion Channel Formation from a Calix[4]arene Amide that Binds HCl. *J. Am. Chem. Soc.* **2002**, *124*, 2267-2278. (b) Seganish, J. L.; Santacroce, P. V.; Salimian, K. J.; Fettinger, J. C.; Zavalij, P.; Davis, J. T. Regulating Supramolecular Function in Membranes: Calixarenes that Enable or Inhibit Transmembrane Cl^- Transport. *Angew. Chem. Int. Ed.* **2006**, *45*, 3334-3338. (c) Izzo, I.; Licen, S.; Maulucci, N.; Autore, G.; Marzocco, S.; Tecilla, P.; Riccardis, F. De Cationic Calix[4]arenes as Anion-Selective Ionophores. *Chem. Commun.* **2008**, 2986-2988. (d) Tong, C. C.; Quesada, R.; Sessler, J. L.; Gale, P. A. *Meso*-Octamethylcalix[4]pyrrole: An Old yet New Transmembrane Ion-pair Transporter. *Chem. Commun.* **2008**, 6321-6323. (e) Wu, X.; Howe, E. N. W.; Gale, P. A. Supramolecular Transmembrane Anion Transport: New Assays and Insights. *Acc. Chem. Res.* **2018**, *51*, 1870-1879. (f) Madhavan, N.; Robert, E. C.; Gin, M. S. A Highly Active Anion-Selective Aminocyclodextrin Ion Channel. *Angew. Chem. Int. Ed.* **2005**, *44*, 7584-7587.
8. (a) Cavallo, G.; Metrangolo, P.; Pilati, T.; Resnati, G.; Sansotera, M.; Terraneo, G. Halogen Bonding: A General Route in Anion Recognition and Coordination. *Chem. Soc. Rev.* **2010**, *39*, 3772-3783. (b) Beale, T. M.; Chudzinski, M. G.; Sarwar, M. G.; Taylor, M. S. Halogen Bonding in Solution: Thermodynamics and Applications. *Chem. Soc. Rev.* **2013**, *42*, 1667-1680. (c) Gilday, L. C.; Robinson, S. W.; Barendt, T. A.; Langton, M. J.; Mullaney, B. R.; Beer, P. D. Halogen Bonding in Supramolecular Chemistry. *Chem. Rev.* **2015**, *115*, 7118-7195. (d) Ballester, P. Experimental Quantification of Anion-π Interactions in Solution Using Neutral Host-Guest Model Systems. *Acc. Chem. Res.* **2013**, *46*, 874-884. (e) Berryman, O. B.; Johnson, D. W. Experimental Evidence for Interactions between Anions and Electron-deficient Aromatic Rings. *Chem. Commun.* **2009**,

3143-3153. (f) Wang, D.-X.; Wang, M.-X. Anion Recognition by Charge Neutral Electron-Deficient Arene Receptors. *Chimia*, **2011**, *65*, 939-943. (g) Giese, M.; Albrecht, M.; Rissanen, K. Experimental Investigation of Anion-π Interactions-Applications and Biochemical Relevance. *Chem. Commun.* **2016**, *52*, 1778-1795. (h) Tepper, R.; Schubert, U. S. Halogen Bonding in Solution: Anion Recognition, Templated Self-Assembly, and Organocatalysis. *Angew. Chem. Int. Ed.* 2**018**, *57*, 6004-6016. (i) Wang, H.; Wang, W.; Jin, W. J. *σ*-Hole Bond vs *π*-Hole Bond: A Comparison Based on Halogen Bond. *Chem. Rev.* **2016**, *116*, 5072-5104.

9. (a) Mareda, J.; Matile, S. Anion-π Slides for Transmembrane Transport. *Chem. Eur. J.* **2009**, *15*, 28-37. (b) Lin, N.-T.; Jentzsch, A. V.; Guénée, L.; Neudörfl, J.-M.; Aziz, S.; Berkessel, A.; Orentas, E.; Sakai, N.; Matile, S. Enantioselective Self-sorting on Planar, π-Acidic Surfaces of Chiral Anion-π Transporters. *Chem. Sci.* **2012**, *3*, 1121-1127. (c) Gorteau, V.; Bollot, G.; Mareda, J.; Perez-Velasco, A.; Matile, S. Rigid Oligonaphthalenediimide Rods as Transmembrane Anion-π Slides. *J. Am. Chem. Soc.* **2006**, *128*, 14788-14789.
10. (a) Wang, X.-D.; Li, S.; Ao, Y.-F.; Wang, Q.-Q.; Huang, Z.-T.; Wang, D.-X. Oxacalix[2]arene[2]triazine based Ion-pair Transporters. *Org. Biomol. Chem.* **2016**, *14*, 330-334. (b) Jentzsch, A. V.; Emery, D.; Mareda, J.; Metrangolo, P.; Resnati, G.; Matile, S. Ditopic Ion Transport Systems: Anion-π Interactions and Halogen Bonds at Work. *Angew. Chem. Int. Ed.* **2011**, *50*, 11675-11678. (c) Adriaenssens, L.; Estarellas, C.; Jentzsch, A. V.; Belmonte, M. M.; Matile, S.; Ballester, P. Quantification of Nitrate-π Interactions and Selective Transport of Nitrate Using Calix[4]pyrroles with Two Aromatic Walls. *J. Am. Chem. Soc.* **2013**, *135*, 8324-8330. (d) Roy, A.; Saha, D.; Mandal, P. S.; Mukherjee, A.; Talukdar, P. pH-Gated Chloride Transport by a Triazine-based Tripodal Semicage. *Chem. Eur. J.* **2017**, *23*, 1241-1247.
11. (a) Jentzsch, A. V.; Emery, D.; Mareda, J.; Nayak, S. K.; Mentrangolo, P.; Resnati, G.; Sakai, N.; Matile, S. Transmembrane Anion Transport Mediated by Halogen-bond Donors. *Nat. Commun.* **2012**, *3*, 905. (b) Jentzsch, A. V.; Matile, S. Transmembrane Halogen-Bonding Cascades. *J. Am. Chem. Soc.* **2013**, *135*,

5302-5303. (c) Lee, L. M.; Tsemperouli, M.; Poblador-Bahamonde, A. I.; Benz, S.; Sakai, N.; Sugihara, K.; Matile, S. Anion Transport with Pnictogen Bonds in Direct Comparison with Chalcogen and Halogen Bonds, *J. Am. Chem. Soc.* **2019**, *141*, 810-814.

12. (a) Ren, C.; Ding, X.; Roy, A.; Shen, J.; Zhou, S.; Chen, F.; Li, S. F. Y.; Ren, H.; Yang, Y. Y.; Zeng, H. A Halogen Bond-mediated Highly Active Artificial Chloride Channel with High Anticancer Activity. *Chem, Sci.* **2018**, *9*, 4044-4051. (b) Ren, C.; Zeng, F.; Shen, J.; Chen, F.; Roy, A.; Zhou, S.; Ren, H.; Zeng, H. Pore-Forming Monopeptides as Exceptionally Active Anion Channels. *J. Am. Chem. Soc.* **2018**, *140*, 8817-8826.
13. (a) Jentzsch, A. V.; Hennig, A.; Mareda, J.; Matile, S. Synthetic Ion Transporters that Work with Anion-π Interactions, Halogen Bonds, and Anion-Macrodipole Interactions. *Acc. Chem. Res.* **2013**, *46*, 2791-2800. (b) Jentzsch, A. V.; Matile, S. Anion Transpor with Halogen Bonds in Halogen Bonding I: Impact on Materals Chemistry and Life Sciences (Eds Mentrangolo, P.; Resnati G.), **2015**.
14. Lovas, S.; He, D. Z. Z.; Liu, H.; Tang, J.; Pecka, J. L.; Hatfield, M. P. D.; K. W. Beisel, Glutamate Transporter Homolog-based Model Predicts that Anion-interaction is the Mechanism for the Voltage-dependent Response of Prestin. *J. Biol. Chem.* **2015**, *290*, 24326-24339.
15. (a) Wang, M.-X. Heterocalixaromatics, New Generation Macrocyclic Host Molecules in Supramolecular Chemistry. *Chem. Commun.* **2008**, 4541-4551. (b) Maes, W.; Dehaen, W. Oxacalix[n](het)arenes. *Chem. Soc. Rev.* **2008**, *37*, 2393-2402. (c) Wang, M.-X. Nitrogen and Oxygen Bridged Calixaromatics: Synthesis, Structure, Functionalization, and Molecular Recognition. *Acc. Chem. Res.* **2012**, *45*, 182-195. (d) Thomas, J.; Rossom, W. V.; Hecke, K. V.; Meervelt, L. V.; Smet, M.; Maes, W.; Dehaen, W. Selenacalix[3]triazines: Synthesis and Host–Guest Chemistry. *Chem. Commun.* **2012**, *48*, 43-45. (e) König, B.; Fonseca, M. H. Heteroatom-Bridged Calixarenes. *Eur. J. Inorg. Chem*. **2000**, 2303-2310.
16. (a) Wang, D.-X.; Zheng, Q.-Y.; Wang, Q.-Q.; Wang, M.-X. Halide Recognition by Tetraoxacalix[2]arene[2]triazine Receptors: Concurrent Noncovalent Halide-π

and Lone pair-π Interactions in Host-Halide-Water Ternary Complexes. *Angew. Chem. Int. Ed.* **2008**, *47*, 7485-7488. (b) Wang, D.-X.; Wang, M.-X. Anion-π Interactions: Generality, Binding Strength, and Structure. *J. Am. Chem. Soc.* **2013**, *135*, 892-897. (c) Wang, D.-X.; Wang, Q.-Q.; Han, Y.; Wang, Y.; Huang, Z.-T.; Wang, M.-X. Versatile Anion-π Interactions between Halides and a Conformationally Rigid Bis(tetraoxacalix[2]arene[2]triazine) Cage and Their Directing Effect on Molecular Assembly. *Chem. Eur. J.* **2010**, *16*, 13053-13057.

17. (a) Xu, R.-B.; Wang, Q.-Q.; Ao, Y.-F.; Li, Z.-Y.; Huang, Z.-T.; Wang, D.-X. Anionic Head Containing Oxacalix[2]arene[2]triazines: Synthesis and Anion-π-Directed Self-Assembly in Solution and Solid State. *Org. Lett.* **2017**, *19*, 738-741. (b) Xu, R.-B.; Wang, Q.-Q.; Ao, Y.-F.; Wang, D.-X. Synthesis of Carboxylate Head-containing Self-complementary Building Units and Their Anion-π Directed Self-assembly. *Supramol. Chem.* **2018**, *30*, 568-574. (c) Tuo, D.-H.; Liu, W.; Wang, X.-Y.; Wang, X.-D.; Ao, Y.-F.; Wang, Q.-Q.; Li, Z.-Y.; Wang, D.-X. Toward Anion-π Interactions Directed Self-assembly with Predesigned Dual Macrocyclic Receptors and Dianions. *J. Am. Chem. Soc.* **2019**, *141*, 1118-1125.
18. Li, S.; Wang, X.-D.; Wang, Q.-Q.; Ao, Y.-F.; Wang, D.-X.; Wang, M.-X. Oxacalix[2]arene[2]triazine Derivatives with Halogen Bond Donors: Synthesis, Structure, and Halide Binding in the Solid State. *Cryst. Growth Des.* **2016**, *16*, 5460-5465.
19. Jentzsch, A. V.; Emery, D.; Mareda, J.; Metrangolo, P.; Resnati, G.; Matile, S. Ditopic Ion Transport Systems: Anion-π Interactions and Halogen Bonds at Work. *Angew. Chem. Int. Ed.* **2011**, *50*, 11675-11678.

Table of Contents